

## Thermo-Mechanical Analysis for Metal Fuel Rod under Transient Operation Condition

Dong Uk Lee, Byoung Oon Lee, Young Gyun Kim, Ki Bog Lee, Jin Wook Jang, Young Il Kim

Korea Atomic Energy Research Institute  
150 Dukjin Dong, Yuseong Ku, Daejeon 305-353, Korea

### Abstract

Computational models for analyzing in-reactor behavior of metallic fuel pins in liquid-metal reactors under transient conditions are developed and implemented in the TRansient thermo-Mechanical Analysis Code for metal fuel rod under transient operation condition (TRAMAC). Not only the basic models for fuel rod performance under transient condition, but also some sub-models used for transient condition are installed in TRAMAC. Among the models, fission gas release model, which takes multibubble size distribution into account to characterize the lenticular bubble shape and the saturation condition on the grain boundary and cladding deformation model have been mainly developed based on the existing models in MACSIS code. Finally, cladding strains are calculated from the amount of thermal creep, irradiation creep, irradiation swelling. The cladding strain model in TRAMAC well predicts the absolute magnitudes and general trends of their predictions compared with those of experimental data. TRAMAC results for FM-1,2,6 pins are more conservative than experimental data and relatively reasonable than those of FPIN2. From the calculation results of TRAMAC, it is apparent that the code is capable of predicting fission gas release, and cladding deformation for LMR metal fuel. The results show that in general, the predictions of TRAMAC agree well with the available irradiation data.

### 1. Introduction

The precise prediction of in-reactor fuel performance during transient overpower as well as steady state operation is essential for the design and licensing of liquid metal reactors. Under transient overpower condition fuel temperature is increased [1]. Exaggerated cladding stresses due to increased fuel cladding mechanical interaction from thermal stresses, differential thermal expansion, transient fuel swelling fuel phase transformation, and incremental gas release may generate breach of the cladding [2].

So far, there has been no dedicated computer code for analyzing in-reactor fuel behavior under transient condition of KALIMER (Korea Advanced Liquid Metal Reactor), whereas MACSIS (Metal fuel performance Analysis Code for Simulating the In-reactor behavior under Steady-state conditions)[3] was developed for analyzing in-reactor behavior and the operation limits of KALIMER fuel under steady state condition. So TRAMAC (Transient Thermo-Mechanical Analysis Code for Metal Fuel Rod under Transient Operation Condition) has been developed to simulate the thermo-mechanical behavior of the metal fuel rod under LMR transient operation condition.

Not only the basic models for fuel rod performance under transient condition, but also some sub-models are installed in TRAMAC. Among the models, FGR and cladding deformation models have been mainly developed based on the existing models in MACSIS code. A series of calculations was carried out to provide the swelling contribution of various bubble growth mechanisms that especially included the transient evolution of fission gas bubble distributions on the grain boundaries of fuel. Existing models in MACSIS were modified to match the transient conditions, and the models were installed into the TRAMAC code. The TRAMAC code predicts the temperature profile, the stress, and the displacements

of fuel rod under transient conditions such as TOP, LOF etc. The validation of the TRAMAC code results has been performed by comparing with results with EBR-II and Whole Pin Furnace (WPF) test data [10].

The objective of this paper is to develop a computer code for KALIMER fuel under transient operation condition, and it is also used as a design tool for the KALIMER fuel development. Section 2 describes major model descriptions in the TRAMAC code. Section 3 shows the transient scenario and input data for the TRAMAC code. Some preliminary results of the transient modeling and benchmark calculations to evaluate the validity of the TRAMAC are given in section 4. Conclusions are given in the final section.

## 2. Code description

### 2.1 Description of transient deformation model for fuel slug

All reactor fuels produce volatile fission products as they produce energy. Even though most of the fission gases produced in fuel matrix are released to the plenum, some are retained within the fuel in the form of bubbles. In the steady-state irradiation, these bubbles achieve an equilibrium condition with the fuel matrix. When the equilibrium between gaseous bubbles and the fuel matrix is upset by some type of off-normal reactor behavior, the fission-gas bubbles can expand or contract to achieve a new state of equilibrium, and the rate at which they can accommodate the new conditions is related to the creep rate of the fuel matrix [4].

The gas swelling model considering this phenomenon gives the strain increments and also calculates fission gas amount released to the gas plenum. This swelling model, which was applicable to analysis of metal swelling including uranium, has been incorporated into the TRAMAC code simulating transient condition. The gas swelling model comprises two parts such as figure 1. One of the sub-models describes migration of fission gas atoms and intragranular gas bubble into the grain or phase boundary. Another model describes growth of the grain-boundary bubbles.

#### 2.1.1 Intra grain diffusion & solid swelling

Swelling is probably the most universal problem encountered in the irradiation of nuclear fuels. The major swelling mechanisms in the fuels are basically the same for all types of fuel; it consists primarily of the nucleation and growth of bubbles of the insoluble fission gases Xe and Kr. In general, the fuels with high thermal conductivity exhibit high fission-gas-induced swelling. This consists of the nucleation and growth of largely immobile intragranular fission gas bubbles, and through the diffusion of fission gas to grain boundaries, in relatively larger intergranular bubbles.

In the intragranular fission gas diffusion model, Booth's classical diffusion theory[5] was directly adopted. His approach contains certain basic assumptions; namely that the entire gas content of the material exists as single, freely diffusing atoms, and that the fissioning substance can be considered to consist of discrete homogeneous spherical particles. Since a discontinuity exists at each particle interface, the surface of each spheroid behaves as a perfect sink for gas atoms. This property defines the boundary condition enabling the solution of the differential equation describing the movement of fission gas within each sphere, and hence, the calculation of the flux of gas atoms through each particle surface. The intragranular gas model calculates the amount of gas atoms and bubbles diffusing into the grain boundary.

Also, assuming that the solid fission product swelling is proportional to local burnup,

$$\Delta \epsilon^{sol} = \dot{\epsilon}^{sol} \cdot \Delta Bu \quad (1)$$

The solid fission product swelling rate was determined from the calculation of volume of all the solid and liquid fission products[13]:

$$\dot{\epsilon}^{sol} = 1.26\% / at\% \quad (2)$$

### 2.1.2 Inter grain bubble behavior & gaseous swelling

The gaseous swelling on grain boundary is a major component of fuel swelling mechanism. Gaseous swelling amount can be estimated by taking multi-bubble size distribution and the saturation condition on the grain boundary into account.

When intragranular bubbles may eventually grow large enough to interconnect, a large amount of swelling has occurred, and therefore, a major fraction of the fission gas will be released from the fuel. While intragranular bubbles achieve an equilibrium condition with the fuel matrix under normal condition, these do not maintain equilibrium between the fuel matrix and internal pressure within bubbles under off-normal condition. This phenomenon under transients reduces fission gas atom density within bubbles, and finally volume of the fuel is rapidly expanded. Allowing a large amount of fuel swelling and gas release to take place reduces fuel-cladding mechanical interaction (FCMI), and is the key to successful high burnup operation of fuels[2].

As described in the reference 6, multi-bubble size distribution on the grain boundary and the average number of bubbles per unit volume at given  $i$  bubble size range,  $\bar{f}_i$ , is estimated by:

$$\int_{n_i}^{n_{i+1}} F(m, \tau, n) dn = \bar{f}_i (n_{i+1} - n_i) \quad (3)$$

or:

$$\bar{f}_i (n_{i+1} - n_i) = 0.23m \cdot \tau^{-4/5} \int_{n_i}^{n_{i+1}} \{ \exp(-A(n\tau^{-2/5} - 0.5)) \times \{ \sinh[B(n\tau^{-2/5} - 0.5)]^{1/2} \} dn$$

where ,  $n_i$  = number of gas atoms in the  $i$  size bubble

$\tau$  = reduced time as a dimensionless parameter

$m' = m_{gb}/E_t$ , the number of gas atoms per unit volume around the grain boundary surface

$m_{gb}$  = number of gas atoms per unit area on the grain boundary

$E_t$  = the effective thickness of grain boundary

$A, B$  = dimensionless constants.

As described in the reference [6], the saturation condition on the grain boundary is estimated by:

$$\frac{1}{4} = \sum_{size\ range} (r_{lb,i})^2 \cdot f_i \quad (4)$$

where ,  $r_{lb,i}$  = longer radius of  $i$  size lenticular bubble on grain boundary

$f_i$  = equivalent number of bubbles at  $i$  size range.

### 2.1.3 The model of fuel core swelling

Fuel deformation is primarily due to retained fission gas bubbles as described in section 2.1.2 , and solid fission product accumulation within the matrix, including liquid phase product. The sum of the volumes of the bubbles trapped on the grain boundary under transient operation condition is determined by considering transient high temperature profile, and the fractional swelling under transient condition is calculated. Finally, swelling caused by solid fission products[3] is added to obtain the total fission-induced swelling. These two mechanisms are incorporated into TRAMAC as follows.

A gas bubble tends to maintain an equilibrium gas pressure by balancing internal gas pressure against bubble surface tension and external pressure. The van der Waals gas law is used to calculate the fission gas swelling. The bubble sizes are defined according to the number of gas atoms. The bubble radius  $r_i$  is given by reference[6]:

$$r_i = [(3kT/8\pi\gamma) n_i]^{1/2} \quad (5)$$

where  $\gamma$  is surface tension of metal fuel,  $0.8 \text{ J/m}^2$ ,  $k$  is Boltzmann constant,  $T$  is temperature (K),  $n_i$  is number of gas atoms in the  $i$  size bubble.

The volume change of fuel slug due to gas swelling is calculated to take into account the multiple-bubble size distribution on the grain boundary. The fractional volume increase due to the accumulation of gas bubbles is given by :

$$\Delta V_s = \sum_{j=1}^{10} \left\{ \left[ \frac{4}{3} \pi n_{i,j} \sum_{i=1}^{10} r_{i,j}^3 \right] / V_j \right\} + f_s \quad (6)$$

where,  $V_j$  is the volume of  $j$  annulus,  $n_{i,j}$  is the number of bubbles in the  $i$  size bubble at  $j$  annulus,  $r_{i,j}$  is the radius of  $i$  size bubble at  $j$  annulus,  $f_s$  is the fractional volume change due to the buildup of solid fission products.

Therefore, the fractional increase in fuel radius due to fuel swelling is given by

$$\Delta D_s \cong r_o \left\{ \frac{0.5 \Delta V_s}{V_o} \right\} \quad (7)$$

where,  $r_o$  is the radius of fuel core,  $V_o$  is initial volume of fuel core.

## 2.2 Description of the cladding deformation model

The deformation of the cladding during transients can be produced by mechanical loading and by metallurgical interaction with the fuel. The primary sources of mechanical loading come from fission gas plenum pressure and Fuel-Cladding Mechanical Interaction (FCMI). Gas pressure loading is dominant for low burnup fuel where the fuel-cladding gap has not closed and for undercooling transients where the cladding tends to expand away from the fuel. FCMI loading of the cladding can occur under Transient Over Power (TOP) conditions where the fuel expands into the cladding. However certain characteristics of metallic fuels tend to minimize this effect. Namely, FCMI can be avoided to high burnup if the as-built smeared density is kept to 75%. These characteristics include the similarities in thermal expansion coefficients between the fuel and the cladding. In addition, the greatest transient cladding deformation usually occurs at the axial location where the cladding temperatures are greatest. This occurs near the top of the fuel column where, in metallic fuel pins, the fuel stresses tend to relax to a hydrostatic state in equilibrium with the plenum pressure[10]. Up to a burnup of 18 at.% in the metallic fuel, it appeared that any contribution to the cladding strain from fuel/cladding mechanical interaction was insignificant. This may be too simplistic for a precise evaluation of FCMI, but it appears adequate for analysis of both steady-state and transient performance[12]. Therefore the predicted major cladding strains under transients are mechanical creep strain caused by differential thermal expansion of fuel and cladding, irradiation-induced creep strain, and irradiation swelling of the cladding itself.

The fuel thermal expansion is computed by finding the volumetric average radial displacement. At each radial node the displacement is computed using the coefficient of thermal expansion given by

$$\alpha^f = \alpha_o^f + \alpha_T^f \times T \quad (8)$$

The thermal expansion of the cladding material (HT9) is computed from the linear function of temperature in the open gap.

$$\frac{\Delta L}{L} = (\alpha_o^c + \alpha_T^c T)(T - T_R) \quad (9)$$

where  $T_R$  is room temperature,  $T$  is the average cladding temperature, and  $\Delta L/L$  is the fraction of length change.

An in-reactor creep equation for HT9 was used as the rate form;  $\dot{\epsilon} = \dot{\epsilon}_I + \dot{\epsilon}_T$ , the term  $\dot{\epsilon}_I$  and  $\dot{\epsilon}_T$  are the irradiation-induced and thermal creep terms of the equation (Kim, 1998). The rate form of the creep equation follows[7].

$$\dot{\epsilon}_I = \left[ B_0 + A \exp\left(-\frac{Q}{RT}\right) \right] \phi \bar{\sigma}^{1.3} \times 10^{-7} \quad (10)$$

where  $\bar{\epsilon}_I$  : effective strain(%),  $\bar{\sigma}$  : effective stress(MPa),  $Q$  : activation energy,  $T$  : temperature(K),  $R$  : gas constant,  $\phi$  : neutron fluence ( $10^{22}$  n/cm<sup>2</sup>,  $E > 0.1$  Mev)

$$\dot{\epsilon}_T = \dot{\epsilon}_{TP} + \dot{\epsilon}_{TS} + \dot{\epsilon}_{TT} \quad (11)$$

Below 600 °C

$$\begin{aligned} \dot{\epsilon}_{TP} &= \left[ C_1 \exp\left(-\frac{Q_1}{RT}\right) \bar{\sigma} + C_2 \exp\left(-\frac{Q_2}{RT}\right) \bar{\sigma}^4 + C_3 \exp\left(-\frac{Q_3}{RT}\right) \bar{\sigma}^{0.5} \right] C_4 \exp(-C_4 t) \\ \dot{\epsilon}_{TS} &= C_5 \exp\left(-\frac{Q_4}{RT}\right) \bar{\sigma}^2 + C_6 \exp\left(-\frac{Q_5}{RT}\right) \bar{\sigma}^5 \\ \dot{\epsilon}_{TT} &= 4C_7 \exp\left(-\frac{Q_6}{RT}\right) \bar{\sigma}^{10} t^3. \end{aligned} \quad (12)$$

For higher temperature

$$\begin{aligned} \dot{\epsilon}_{TP} &= \left[ C_1 \exp\left(-\frac{Q_1}{RT}\right) \bar{\sigma} + C_2 \exp\left(-\frac{Q_2}{RT}\right) \bar{\sigma}^4 + C_3 \exp\left(-\frac{Q_3}{RT}\right) \bar{\sigma}^{0.5} \right] C_4 (1 - \exp(-C_4 t)) \\ \dot{\epsilon}_{TS} &= \left[ C_5 \exp\left(-\frac{Q_4}{RT}\right) \bar{\sigma}^2 + C_6 \exp\left(-\frac{Q_5}{RT}\right) \bar{\sigma}^5 \right] t \\ \dot{\epsilon}_{TT} &= C_7 \exp\left(-\frac{Q_6}{RT}\right) \bar{\sigma}^{10} t^4 \end{aligned} \quad (13)$$

where  $\dot{\epsilon}_{TP}$  : thermal primary creep strain rate(%/s),  $\dot{\epsilon}_{TS}$  : thermal secondary creep strain rate(%/s),  $\dot{\epsilon}_{TT}$  : thermal tertiary creep strain rate(%/s),  $\bar{\sigma}$  : effective stress(MPa),  $t$ : time in seconds.

Values for the constants in these equations are :

$$\begin{aligned} R &= 1.986 \text{ cal/}^{\circ}\text{K mole (gas constant)} \\ B_0 &= 1.38 \times 10^{-4} \\ A &= 2.59 \times 10^{14} \\ Q &= 73,000 \\ C_1 &= 13.4, \\ C_2 &= 8.43 \times 10^{-3} & Q_1 &= 15,027 \\ C_3 &= 4.08 \times 10^{18} & Q_2 &= 26,451 \\ C_4 &= 1.6 \times 10^{-6} & Q_3 &= 89,167 \\ C_5 &= 1.17 \times 10^9 & Q_4 &= 83,142 \end{aligned}$$

$$C_6 = 8.33 \times 10^9 \quad Q_5 = 108,276$$

$$C_7 = 9.53 \times 10^{21} \quad Q_6 = 282,700.$$

Swelling is generally the function of the fluence and expressed bilinear equation. HT9 may never show significant swelling, regardless of fluence, although transmission electron microscopy has revealed a few voids at low temperature ( $\sim 400^\circ\text{C}$ )[8].

$$\frac{\Delta V}{V} = S_0 + D \quad (14)$$

where  $S_0$  is the fractional volume change due to void formation and  $D$  is the fractional volume change due to solid state reactions.

$$S_0 = (0.01)R \left[ \phi t + \frac{1}{\alpha} \ln \left\{ \frac{1 + \exp[\alpha(\tau - \phi t)]}{1 + \exp(\alpha\tau)} \right\} \right] \quad (15)$$

$$D = (0.01)(0.15)[1 - \exp(-0.1\phi t)]$$

where  $R = 0.085 \exp[-1 \times 10^{-4}(T - 400)^2]$

$\tau = 14.2$ , Incubation Parameter,  $(10^{22} \text{ n/cm}^2, E > 0.1 \text{ MeV})$

$\alpha = 0.75$ , Curvature parameter,  $(10^{22} \text{ n/cm}^2)^{-1}$

$\phi t = \text{Noutron fluence, } 10^{22} (\text{n/cm}^2)^{-1}$

### 3. Transient Scenario and Input Data

This study will concentrate on cladding deformation and its integrity, which are of fundamental concern because the cladding provides the primary barrier to the release of radionuclides. Cladding damage during accident transients is a strong function of cladding temperature. For design basis accident (DBA) transients including scram-protected transient overpower (TOP), loss-of-flow (LOF) and loss-of-heat sink (LOHS) events, the thermal response of the cladding for these transients can generally be characterized by a temperature ramp of  $1\text{-}100^\circ\text{C/s}$  followed by reactor scram and rapid cooling within 10-20 seconds after accident initiation[10].

One of the key phases in the development of the code for analyzing transient fuel behavior is validation of the code's predictions through comparison of calculated results with results of experiments on metallic fuels. Tests on intact transient fuel pins include in-reactor tests in the EBR-II reactor, and out-of-reactor Whole Pin Furnace (WPF) test[10] which has been developed to span the range between the TREAT and the EBR-II test regimes.

Six WPF tests have been conducted using IFR metallic fuel pins irradiated in EBR-II[10]. Rods evaluated in this study are FM-1,2,6 rods, which equal to unity in plenum & fuel volume ratio. Key pin parameters and test conditions for FM-1,2,6 rods are summarized in table 1. The TRAMAC uses the pretransient performance characterization (geometry, fission gas release, fuel restructuring, etc.) for the test pin provided by MACSIS which is a computer program for simulating the behavior of the metal fuel rods for a liquid metal cooled reactor under normal operating conditions. This was done to minimize the influence of the assumed pretransient condition of the pin on the comparisons of the code predictions for the test. The TRAMAC also needs the input data such as the same cladding surface temperatures based on the planned peak cladding temperature and the axial temperature profile determined from measured furnace characteristics.

FM-1 and FM-2 experiments were ramp-and-hold test with the peak-cladding temperature ramped from  $500^\circ\text{C}$  to the test temperature at  $6^\circ\text{C/s}$ , followed by a hold at the test temperatures ( $820, 660^\circ\text{C}$ ) duration 67 and 112 minutes until the signal of fuel pin failure was detected. Also test FM-6 was run in two stages of ramp-and-hold test at nominal peak cladding temperatures of  $650\text{-}670^\circ\text{C}$  ( $650^\circ\text{C}$  at the fuel top,  $670^\circ\text{C}$  in the plenum). Stage 1 of the test was run for 12 hours, just after which the pin was removed from the test section to

measure the incremental diametral strains. The pin was then inserted back into the furnace and run for another 24 hours [10].

#### 4. Benchmark Calculations and Discussion

To evaluate the predictive capability of TRAMAC, it needs to compare the calculation results of cladding strain by TRAMAC with the WPF experimental results.

For the comparison of the predictions for cladding deformation with the experimental data, the test results for FM-1,2,6 test rods were used, which were irradiated at the Experimental Breeder Reactor II by ANL until 3 at.% and then have conducted test at WPF (Whole Pin Furnace). The WPF testing facility uses a computer-controlled radiant furnace, which is able to heat intact irradiated fuel pins up to the temperature point of cladding breach.

For FM-1, the TRAMAC code predicted peak cladding strain 4.59% during 67 minutes as shown in the figure 2-a. The prediction by TRAMAC is higher than that of experimental data. This result is more conservative than experimental data (3.3%) with the failure time 67 minutes. However, it is apparent that the prediction by the TRAMAC code is in slightly better agreement with the experiments than that (6%) of FPIN2. Based on transient plastic flow law, 6% of strain can be applied as a strain criterion of fuel rod under transient condition. According to this criterion, the FPIN2 exceeded the criterion at only 36 minutes and the fuel pin was failed. For FM-2, it is appeared that TRAMAC result exceeds the peak strain 6% within about 50 minutes as shown in the figure 3-a. This result also is more conservative than experimental data (4.3%) with the failure time 112 minutes. FPIN2 predicts only 42 minutes of time to fail, which is much lower than that of experiment data.

For FM-6, TRAMAC predicted peak cladding strain 1.42% during 1274 minutes as shown in the figure 4-a. This result also is more conservative than experimental data (0.89%) without failure during 1260 minutes. FPIN2 predicts only 270 minutes of time to fail, which is much lower than that of experiment data.

For irradiation temperatures less than 540 °C, as in-reactor creep data are consistent with a stress exponent of  $1 \leq n < 2$ , creep is relatively insensitive to temperature but it getting sensitive to the temperature range higher than 570 °C. And for the temperature range higher than 650 °C, HT9 alloy no longer displays the in-reactor creep resistance that it exhibited at irradiation temperatures less than 570 °C, since the HT9 in-reactor creep increases with a stress exponent of the order 3 to 7[11]. Therefore as shown in the figure 2-b~d and 3-b~d, total cladding strain is affected by irradiation swelling with a linear fluence dependence because the cladding temperatures are less than 650 °C under steady-state condition. When cladding temperature exceeds 650 °C under transient condition, the thermal creep mechanisms dominate the in-reactor creep behavior of HT9.

As stated above, TRAMAC results for FM-1,2,6 pins are in slightly better agreement with the experiments than those of FPIN2. The predictions of TRAMAC are more conservative than experimental data and relatively reasonable than those of FPIN2. In other words, TRAMAC predicted shorter failure times and slightly larger plastic strain than experimental data. The cladding strains predicted by TRAMAC seem to agree well with the trend. The foregoing comparisons show that TRAMAC is capable of efficiently simulating in-reactor behavior of metallic fuel under transient events.

#### 5. Conclusions

The precise prediction of in-reactor fuel performance during transient overpower as well as steady state operation is essential for the design and licensing of liquid metal reactors.

The TRAMAC simulating transient conditions have been successfully developed for metal fuel in KALIMER. Not only the basic models for fuel rod performance under transient condition, but also some sub-models used for transient condition are installed in TRAMAC. Among the models, the semi-theoretical fission gas release and cladding deformation models have been mainly developed based on the existing models in MACSIS code. The validation of the TRAMAC code was evaluated by comparing the available experimental data.

The cladding strain model in TRAMAC well predicts the absolute magnitudes and general trends of their predictions compared with those of experimental data. From the calculation results of TRAMAC, it is apparent that the code is capable of predicting fission gas release, and cladding deformation for LMR metal fuel under transient condition. Therefore, a general potential of TRAMAC as a calculational tool to evaluate the integrity of metal fuel under transient operation conditions is identified.

#### Acknowledgements

This project has been carried out under the Long-Term R&D Program supported by the Ministry of Science and Technology (MOST) of Korea.

#### Reference

- [1] T.S. Roth, A. Biancheria, Proceeding ANS International Conference on Reliable Fuels for LMRs, 1986.
- [2] R.W. Cahn et al., Material Science and Technology, Volume 10 A, Nuclear Material Part I. VCH Publishers Inc., New York, 1994.
- [3] W. Hwang et al., Nuclear Technology 123, 130, 1998.
- [4] G.L. Hofman et al., Metallurgical Transactions A 21A, 517, 1990.
- [5] A.H. Booth, CRDC-721, Atomic Energy of Canada Limited, 1957.
- [6] W. Hwang, H.C. Suk, Nuclear Technology 95, 314, 1991.
- [7] K.G. Kim et al., FD100-DB-01-98, Korea Atomic Energy Research Institute, 1998.
- [8] D.S. Gelles, J. Nucl. Mater. 122&123, 207, 1984.
- [9] J.L. Straalsund, D.S. Gelles, HEDL-SA-2771.
- [10] J.M. Kramer et al., J. Nucl. Mater. 204, 203, 1993.
- [11] R.J. Puigh, G.L. Wire, Topical Con. On Ferritic Alloys for Use in Nuclear Energy Technology, Utah, USA, 1983.
- [12] G.L. Hofman et al., Progress in Nuclear Energy 31, 83, 1997.
- [13] W. Hwang et al., Proceedings of the Korean Nuclear Society Spring Meeting, Korea, 1998.

Table 1. Test condition for FM-1,2,6 rod and test results

Test no.	Fuel Type	Cladding type	Plenum fuel vol. Ratio	Burnup (a/o)	Test temp. (°C)	Test duration (min)	Failure time(min)	Peak strain(%)
FM-1	U-10Zr	HT9	1.0	3.0	820	67	67	3.3
FM-2	U-19Pu-10Zr	HT9	1.0	3.0	820	112	112	2.3-4.3
FM-6	U-19Pu-10Zr	HT9	1.0	11.3	650~670	2160	No failure	0.89

Table 2. Comparison of calculation and test results

	FM-1		FM-2		FM-6	
	Peak Strain	Time	Peak Strain	Time	Peak Strain	Time
FPIN	6	36	6	42	6	270
LIFE	1.1	79*	~1	75	1.03	1320**
TRAMAC	4.59	67	5.946	~49	1.42	2174
TEST	3.3	67	2.3-4.3	112	0.89	2160

\* Transient creep-rupture correlation

\*\* Steady- state creep-rupture correlation

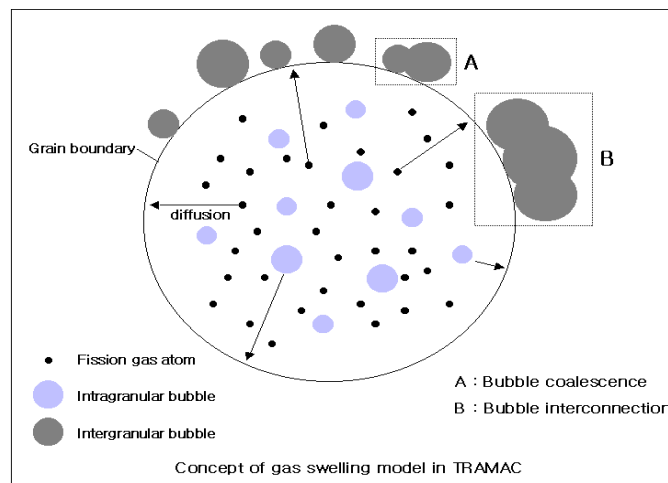


Figure 1. Concept of fission gas swelling model in TRAMAC

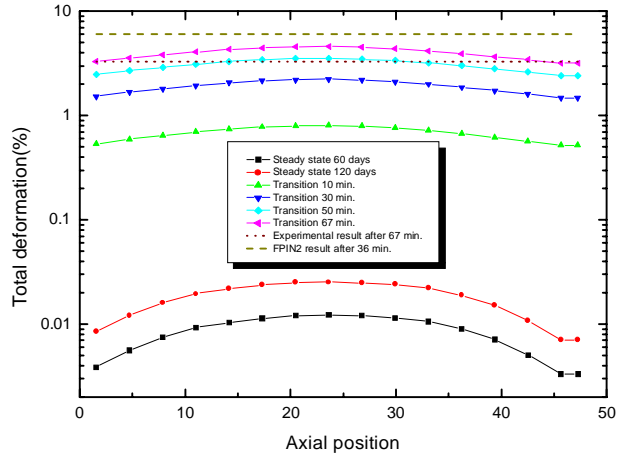


Figure 2-a. TRAMAC prediction of cladding strain for FM-1 rod

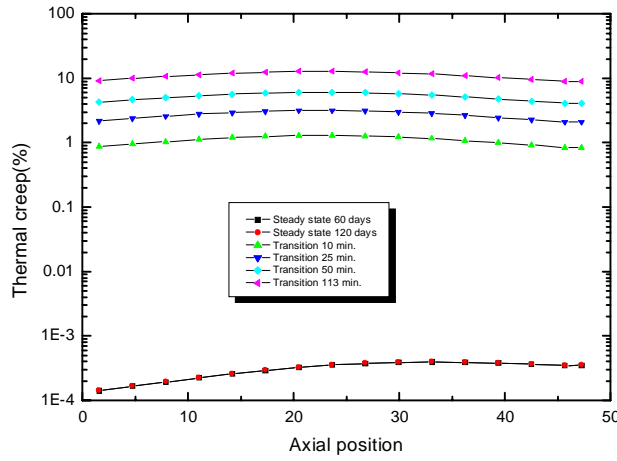


Figure 2-b. TRAMAC prediction of thermal creep for FM-1 rod

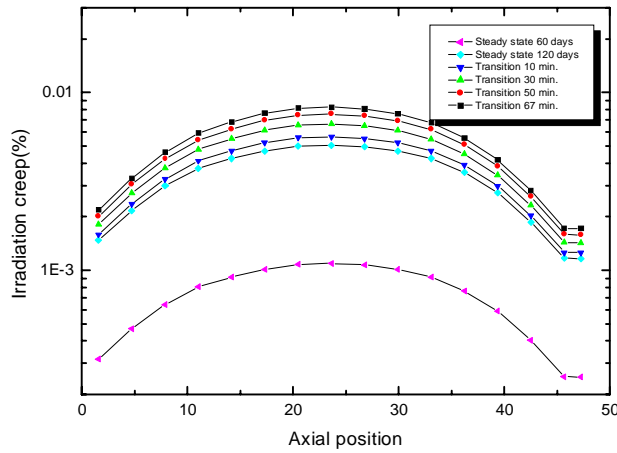


Figure 2-c. TRAMAC prediction of irradiation creep for FM-1 rod

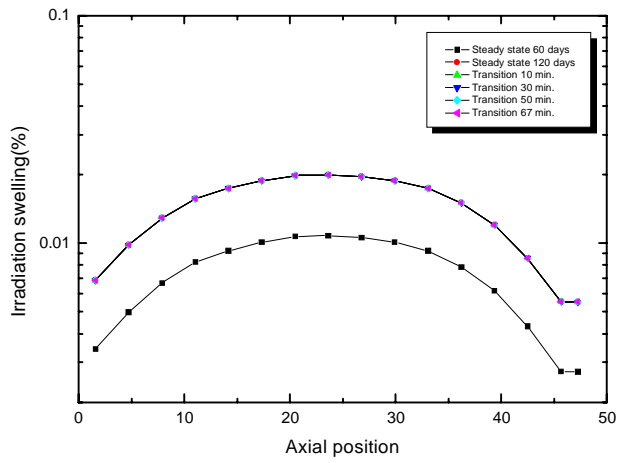


Figure 2-d. TRAMAC prediction of cladding irradiation swelling for FM-1 rod

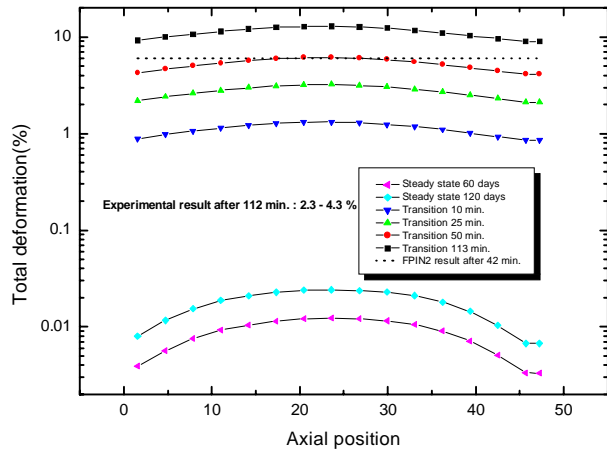


Figure 3-a. TRAMAC prediction of total cladding strain for FM-2 rod

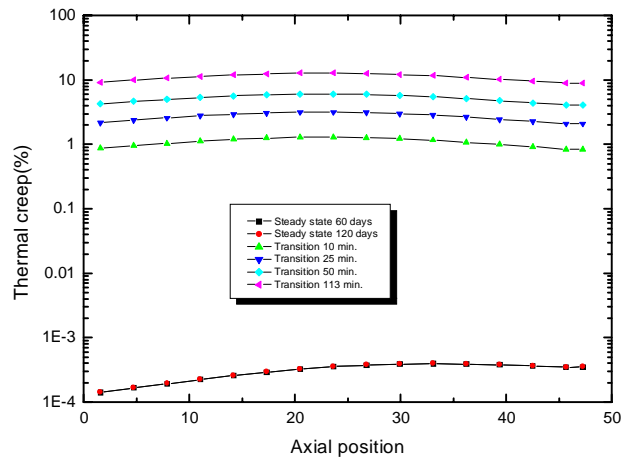


Figure 3-b. TRAMAC prediction of thermal creep for FM-2 rod

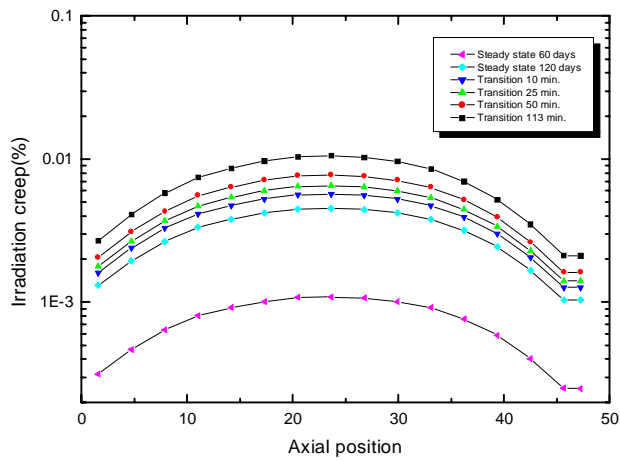


Figure 3-c. TRAMAC prediction of irradiation creep for FM-2 rod

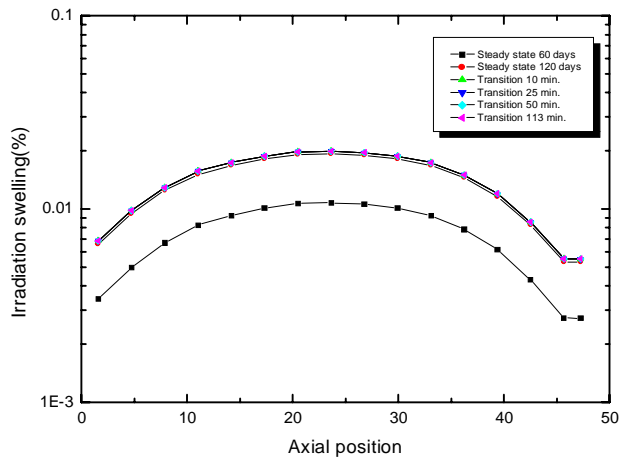


Figure 3-d. TRAMAC prediction of irradiation cladding swelling for FM-2 rod

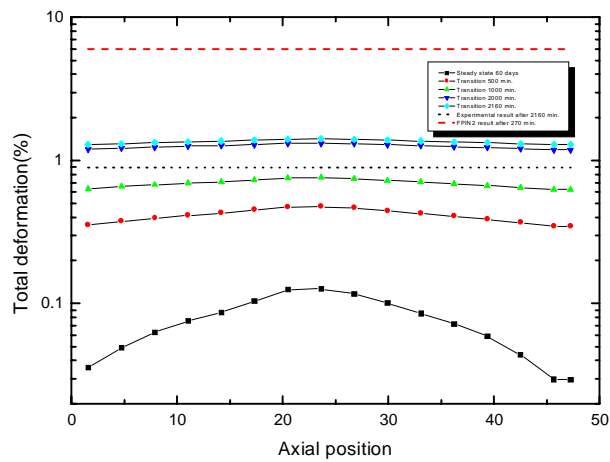


Figure 4-a. TRAMAC prediction of total cladding strain for FM-6 rod

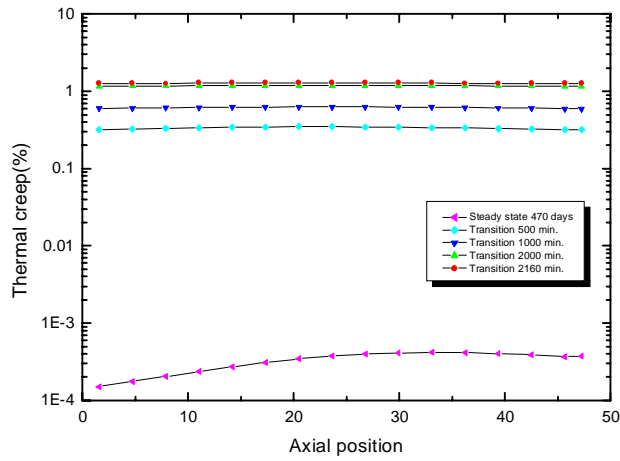


Figure 4-b. TRAMAC prediction of thermal creep for FM-6 rod

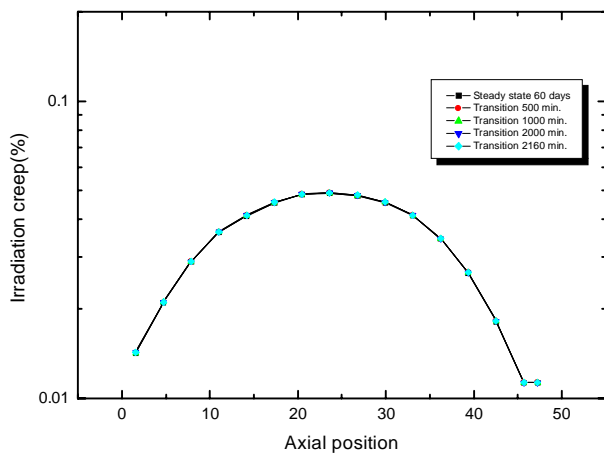


Figure 4-c. TRAMAC prediction of irradiation creep for FM-6 rod

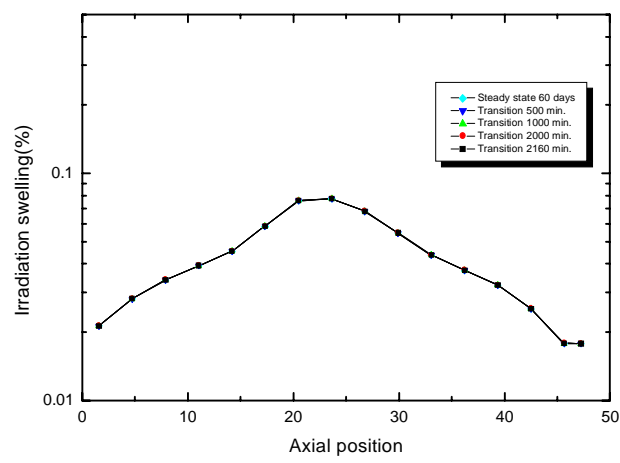


Figure 4-d. TRAMAC prediction of irradiation cladding swelling for FM-6 rod